

X-ray absorption and optical spectroscopy studies of (Mg_{1-x}Al_x)B₂

H. D. Yang¹, H. L. Liu², J.-Y. Lin³, M. X. Kuo², P. L. Ho¹, J. M. Chen⁴, C. U. Jung⁵,
Min-Seok Park⁵, and Sung-Ik Lee⁵

¹*Department of Physics, National Sun Yat-Sen University, Kaohsiung 804, Taiwan ROC*

²*Department of Physics, National Taiwan Normal University, 88, Sec. 4, Ting-Chou Road,
Taipei 116, Taiwan ROC*

³*Institute of Physics, National Chiao Tung University, Hsinchu 300, Taiwan ROC*

⁴*Synchrotron Radiation Research Center (SRRC), Hsinchu 300, Taiwan ROC*

⁵*National Creative Research Initiative center for Superconductivity and Department of Physics,
Pohang University of Science and Technology, Pohang 790-784, Republic of Korea*

(November 5, 2018)

Abstract

X-ray absorption spectroscopy and optical reflectance measurements have been carried out to elucidate the evolution of the electronic structure in (Mg_{1-x}Al_x)B₂ for $x = 0.0, 0.1, 0.2, 0.3,$ and 0.4 . The important role of B $2p$ σ hole states to superconductivity has been identified, and the decrease in the hole carrier number is *quantitatively* determined. The rate of the decrease in the hole concentration agree well with the theoretical calculations. On the other hand, while the evolution of the electronic structure is gradual through the doping range, T_c suppression is most significant at $x = 0.4$. These results suggest that the superstructure in (Mg_{1-x}Al_x)B₂, in addition to the σ holes, can affect the lattice dynamics and contributes to the T_c suppression effect. Other possible explanations like the topological change of the σ band

Fermi surface are also discussed.

PACS numbers: 74.25.Gz, 74.70.Ad, 74.25.Jb, 78.70.DM

Within two years of the discovery of superconductivity in MgB_2 [1], intensive studies have led to tremendous understanding of this new and unique intermetallic superconductor. The main frame has been set both by theory and experiments. MgB_2 is a phonon-mediated strong coupling superconductor. The two-dimensional B $2p$ σ holes play a crucial role in superconductivity of MgB_2 [2–5]. In contrast to classical s -wave superconductors, MgB_2 has multiple superconducting energy gaps though it is fully gapped [2,5–10]. However, there are issues on MgB_2 remaining somewhat open yet. One example is the Al doping effects on T_c of MgB_2 . It is established that the Al doping leads to T_c suppression in MgB_2 . Al doping also shortens the c axis in the layered hexagonal structure. Furthermore, the Al-layer ordering in $(\text{Mg}_{1-x}\text{Al}_x)\text{B}_2$ was reported [11,12]. Since superconductivity in MgB_2 is of phonon origin, the interplay of the lattice dynamics and the evolution of the electronic structure in $(\text{Mg}_{1-x}\text{Al}_x)\text{B}_2$ is of great interest. However, compared to the detailed studies of phonon spectrum in $(\text{Mg}_{1-x}\text{Al}_x)\text{B}_2$ [13], the Al doping effects on the electronic structure have not been thoroughly explored yet. In this paper, we report detailed x-ray absorption and optical reflectance measurements in $(\text{Mg}_{1-x}\text{Al}_x)\text{B}_2$ for $x = 0.0, 0.1, 0.2, 0.3,$ and 0.4 . Comparisons between the present results and other theoretical and experimental works provide deeper insight into the electronic structure and T_c suppression mechanism in $(\text{Mg}_{1-x}\text{Al}_x)\text{B}_2$.

To prepare $(\text{Mg}_{1-x}\text{Al}_x)\text{B}_2$, the stoichiometric mixture of Mg, ^{11}B , and Al powder (Alfa Aesar) was ground softly for an hour. Resultant powder was palletized and wrapped by a Ta foil. Then it was put into a high pressure cell. This whole process was performed in an inert Ar gas. A 12 mm cubic multi-anvil system was used for a high pressure synthesis. The cell was heated up to 950°C and maintained 950°C for 2 hours. Then it was quenched to room temperature. Details of high-pressure synthesis will be found elsewhere [14,15]. The lattice parameters a and c , shown in the inset of Fig. 1, were obtained from x-ray diffraction measurements. Al doping led to an obvious decrease in c due to the smaller ionic radius of Al^{3+} than that of Mg^{2+} , while the effect on a was relatively insensitive. The diffraction pattern of the $x = 0.2$ sample showed the presence of two phases. All the above

x-ray diffraction results were consistent with those in the literature [11,12]. The resistivity ρ was measured by the four-probe method, as shown in Fig. 1. T_c was determined by the midpoint of the transition, and was consistent with the magnetization M measurements. The sharp transition both in ρ and M manifested the good quality of the samples. Moreover, T_c suppression effects due to Al doping are consistent with the reported results [11,12].

X-ray absorption near edge structure (XANES) in fluorescence mode is a powerful tool to investigate the unoccupied (hole) electronic states in complex materials and is bulk sensitive. The B K -edge x-ray absorption spectra were carried out using linear polarized synchrotron radiation from 6-m high-energy spherical grating monochromator beamline located at SRRC in Taiwan. Details of the measurements were described elsewhere [16,17]. Energy resolution of the monochromator is set to be 0.15 eV for the B K -edge energy range. The energy was calibrated as in Ref. [18]. The absorption spectra were normalized to the maximum of the peak around 200 eV.

Near-normal optical reflectance spectra were taken at room temperature on mechanically polished surfaces of high density polycrystalline samples. Middle infrared (600-3000 cm^{-1}) measurements were made with a Perkin-Elmer 2000 spectrometer coupled with a FT-2R microscope, while the spectra in the near-infrared to near-ultraviolet regions (4000-55000 cm^{-1}) were collected on a Perkin-Elmer Lambda-900 spectrometer. The modulated light beam from the spectrometer was focused onto either the sample or an Au (Al) reference mirror, and the reflected beam was directed onto a detector appropriate for the frequency range studied. The different sources and detectors used in these studies provided substantial spectral overlap, and the reflectance mismatch between adjacent spectral ranges was less than 1 %.

The B K -edge XANES on $(\text{Mg}_{1-x}\text{Al}_x)\text{B}_2$ was studied and shown in Fig. 2. The peaks centered between 186.5 and 187 eV can be identified to be closely associated with B $2p$ σ holes. Two additional peaks around 192~194 eV (not shown), probably due to either boron oxides or resonances, were also observed in this work. These features do not appear to affect the peak of B $2p$ σ states, and are not included in the following discussions [18-20].

The most noticeable change is the decrease in the intensity of the pre-edge peak with increasing Al doping. This can be reasoned as the electron doping effect with the substitution of Al^{3+} for Mg^{2+} . XANES thus directly verifies the crucial role of B $2p$ σ holes together with T_c suppression effects due to Al doping. It is also noticed that the change of the intensity is gradual, like the x dependence of $T_c(x)$, until $x = 0.4$. No dramatic change between $x = 0.0$ and 0.1 was observed in the present work, while a 65% drop in the spectral weight was reported in Ref. [20]. In general, the onset and the peak energies both increase with Al doping as expected naively by the concept of hole filling, while indicating that the rigid band model can not be vigorously applied. Furthermore, the onset and the peak energies actually decrease slightly from $x = 0.0$ to 0.1 , which probably suggests a corresponding change of the core level energy. This curious tendency appears to be genuine, since it was also observed in another independent work [21].

To further quantify the decrease in the number of hole carriers, the optical spectroscopy has been proved to be an effective tool for the investigation of the doping-induced spectral weight [22]. The optical properties (*i.e.* the complex conductivity $\sigma(\omega) = \sigma_1(\omega) + i\sigma_2(\omega)$ or dielectric function $\epsilon(\omega) = 1 + 4\pi i\sigma(\omega)/\omega$) were calculated from Kramers-Kronig analysis of the reflectance data [23]. To perform these transformations one needs to extrapolate the reflectance at both low and high frequencies. At low frequencies the extension was done by modeling the reflectance using the Drude model and using the fitted results to extend the reflectance below the lowest frequency measured in the experiment. The high-frequency extrapolations were done by using a weak power law dependence, $R \sim \omega^{-s}$ with $s \sim 1-2$.

Similar optical experiments has been performed on MgB_2 [24]. In this work, the detailed optical measurements on $(\text{Mg}_{1-x}\text{Al}_x)\text{B}_2$ are reported. Figure 3 shows the room-temperature real part of the optical conductivity $\sigma_1(\omega)$ as a function of Al doping, obtained from a Kramers-Kronig transformation of the measured reflectance data. For the $x = 0.0$ sample, the optical conductivity can be described in general terms as (i) coherent response of itinerant charge carries at zero frequency; (ii) an overdamped mid-infrared component around 3500 cm^{-1} ; and (iii) two interband transitions near 17000 and 50000 cm^{-1} . We have tried to fit

the conductivity spectrum in the whole frequency range with a Drude part and three Lorentz oscillators. The Drude plasma frequency of the carriers ω_{pD} and their scattering rate $1/\tau_D$ are 27000 and 1000 cm^{-1} , respectively. The estimated Drude resistivity [$\rho_{\text{Drude}} = (\omega_{pD}^2 \tau_D / 60)^{-1}$, in unit $\Omega\text{-cm}$] is $8 \times 10^{-5} \Omega\text{-cm}$, in reasonable agreement with the transport results. As Al doping proceeds, the far-infrared conductivity is decreasing, while the oscillator strength of the mid-infrared absorption is nearly independent of doping.

An attempt in separating the zero-frequency absorption channel from the mid-infrared absorption sometimes produced ambiguous results. This is the case that there has been much discussion over the one-component and the two-component pictures to describe the optical conductivity of high- T_c cuprates [25]. The doping dependence of the low-frequency optical conductivity of these samples can also be summarized by plotting the integrated spectral weight in the conductivity [23],

$$N_{\text{eff}}(\omega) = \frac{2m_0 V_{\text{cell}}}{\pi e^2} \int_0^{\omega} \sigma_1(\omega') d\omega', \quad (2)$$

where m_0 is taken as the free-electron mass, and V_{cell} is the unit cell volume. $N_{\text{eff}}(\omega)$ is proportional to the number of carriers participating in the optical absorption up to a certain cutoff frequency ω , and has the dimension of frequency squared. Integration of the conductivity up to $\omega = 8000 \text{ cm}^{-1}$ - the frequency at which we observe a clear onset of interband transitions-provides only 30% of the spectral weight we measure when ω is extended up to our experiment limit of 52000 cm^{-1} . Fig. 4 shows the quantity $N_{\text{eff}}(\omega = 8000 \text{ cm}^{-1})$ plotted as a function of T_c , illustrating the correlation between the number of carriers and T_c in the $(\text{Mg}_{1-x}\text{Al}_x)\text{B}_2$ systems. It is interesting to note that the spectral weight corresponds to an effective number of carriers of ~ 0.48 and 0.16 for the $x = 0.0$ and 0.4 samples, suggesting that each Al removes approximately one carrier. From Fig. 4, it is intriguing to note that T_c changes accordingly with N_{eff} until a more significant drop in T_c occurs at $x = 0.4$. This implies that an additional effect other than N_{eff} begins to play a role in the determination of T_c at the composition of $x = 0.4$. Another intriguing plot is N_{eff} vs x as in Fig. 5. It unambiguously demonstrates *no* abrupt change of N_{eff} at either $x = 0.1$

or 0.4, in agreement with XANES in Fig. 3. It has been argued that the evolution of the electronic structure is responsible for the change of the lattice dynamics in $(\text{Mg}_{1-x}\text{Al}_x)\text{B}_2$ [13]. The results in Figs. 4 and 5 further suggest that the phonon spectrum could be affected by the superstructure, in addition to the factor of N_{eff} . Why this superstructure effect takes place at $x = 0.4$ rather than at smaller x is unknown. Perhaps the composition of $x = 0.4$ approaches $x = 0.5$ close enough where the Al layer ordering is much preferred. The formation of the superstructure has been explained recently by a simple model, though with a too low instability temperature for the phase separation [26]. The interplay of the electronic structure, the lattice dynamics, and the superstructure still remains unclear with respect to the details.

B $2p$ σ holes in $(\text{Mg}_{1-x}\text{Al}_x)\text{B}_2$ were actually theoretically investigated [4]. Figure 5 provides an excellent stage to compare between theoretical calculations and experimental results. Though the absolute value of the carrier number is difficult to compare, the comparison of the relative change of the carrier number due to Al doping can be made. Theoretical calculations predict $N_{\text{eff}}(x)/N_{\text{eff}}(0)=1-1.75x$ [4], which amazingly agrees with the experimental results in Fig. 5. It is noted that the solid line in Fig. 5 represents the theoretical prediction *with no fitting parameter*. This astonishing agreement deserves further consideration. In the calculations of Ref. [4], doped Al atoms were assumed to be distributed in Mg planes, and no superstructure effects were included. It seems that the occurrence of the superstructure has no effect on N_{eff} while it affects the lattice dynamics which contributes to further T_c suppression for $x \geq 0.4$. This scenario is qualitatively in accord with the experimental results [13]. It is also likely that the coupling between σ and π bands has to be included to account for the correct T_c suppression effects [26]. Furthermore, another first principle calculation work (without considering the superstructure effects) suggests that an abrupt topological change in the σ Fermi surface between $x=0.3$ and 0.4 [27]. How this electronic structure change reconciles with the observed smooth change of XANES and $N_{\text{eff}}(x)$, and how it is related to the evolution of the lattice dynamics and the T_c suppression remain largely unknown. Certainly further theoretical studies as in Ref. [4] but including the

interplay of all the electronic structure, the lattice dynamics, and the superstructure effects are indispensable.

To conclude, spectroscopy studies of $(\text{Mg}_{1-x}\text{Al}_x)\text{B}_2$ by XANES and optical reflectance measurements not only identify the importance of B $2p$ σ hole states to superconductivity, but also quantify the changes of the carrier number due to Al doping. The quantitative decreasing rate of the σ hole number agrees well with the theoretical calculations. No abrupt change of the carrier number was observed for $x = 0.0$ to 0.4 . This smooth change is difficult to reconcile with the large T_c suppression at $x=0.4$. While either the superstructure or the topological change of the electronic structure in $(\text{Mg}_{1-x}\text{Al}_x)\text{B}_2$ could be responsible for this anomaly, the experimental results of the electronic structure evolution indicate that a full understanding of the large T_c suppression at $x = 0.4$ is still desirable.

ACKNOWLEDGMENTS

We are grateful to B. Renker and R. Heid for inspiring discussions in MOS2002 conference. This work was supported by the National Science Council of the Republic of China under Grant Nos. NSC 91-2112-M-003-021, NSC91-2112-M-110-005 and NSC91-2112-M-009-046.

REFERENCES

- [1] J. Nagamatsu, N. Nakagawa, T. Muranaka, Y. Zenitani, and J. Akimitsu, *Nature* **410**, 63 (2001).
- [2] A. Y. Liu, I. I. Mazin, and J. Kortus, *Phys. Rev. Lett.* **87**, 087005 (2001).
- [3] P. P. Singh, *Phys. Rev. Lett.* **87**, 087004 (2001).
- [4] S. Suzuki, S. Higai, and K. Nakao, *J. Phys. Soc. Jpn.* **70**, 1206 (2001).
- [5] H. J. Choi, D. Roundy, H. Sun, M. L. Cohen, and S. G. Louie, *Nature* **418**, 758 (2002).
- [6] H. D. Yang, J.-Y. Lin, H. H. Li, F. H. Hsu, C.-J. Liu, S.-C. Li, R.-C. Yu and C.-Q. Jin, *Phys. Rev. Lett.* **87**, 167003 (2001).
- [7] F. Bouquet, R. A. Fisher, N. E. Phillips, D. G. Hinks, and J. D. Jorgensen, *Phys. Rev. Lett.* **87**, 047001 (2001).
- [8] T. Takahashi, T. Sato, S. Souma, T. Muranaka, and J. Akimitsu, *Phys. Rev. Lett.* **86**, 4915 (2001).
- [9] S. Tsuda, T. Yokoya, T. Kiss, Y. Takano, K. Togano, H. Kito, H. Ihara, and S. Shin, *Phys. Rev. Lett.* **87**, 177006 (2001).
- [10] X. K. Chen, M. J. Konstantinović, J. C. Irwin, D. D. Lawrie, and J. P. Franck, *Phys. Rev. Lett.* **87**, 157002 (2001).
- [11] J. S. Slusky, N. Rogado, K. A. Regan, M. A. Hayward, P. Khalifah, T. He, K. Inumaru, S. Loureiro, M. K. Hass, H. W. Zandbergen, and R. J. Cava, *Nature* **410**, 343 (2001).
- [12] J. Q. Li, L. Li, F. M. Liu, C. Dong, J. Y. Xiang, and Z. X. Zhao, *Phys. Rev. B* **65**, 132505 (2002).
- [13] B. Renker, K. B. Bohnen, R. Heid, D. Ernst, H. Schober, M. Koza, P. Adelman, P. Schweiss, and Th. Wolf, *Phys. Rev. Lett.* **88**, 067001 (2002), and references therein.

- [14] C. U. Jung, Min-Seok Park, W. N. Kang, Mun-Seog Kim, Kijoon H. P. Kim, S. Y. Lee, and Sung-Ik Lee, *Appl. Phys. Lett.* **78**, 4157 (2001).
- [15] C. U. Jung, Heon-Jung Kim, Min-Seok Park, Mun-Seog Kim, J. Y. Kim, Zhonglian Du, Sung-Ik Lee, K. H. Kim, J. B. Betts, M. Jaime, A. H. Lacerda, and G. S. Boebinger, *Physica C* **377**, 21 (2002).
- [16] J. M. Chen, R. S. Liu, J. G. Lin, C. Y. Huang, and J. C. Ho, *Phys. Rev. B* **55**, 14586 (1997).
- [17] I. P. Hong, J.-Y. Lin, J. M. Chen, S. Chatterjee, S. J. Liu, Y. S. Gou, and H. D. Yang, *Europhys. Lett.* **58**, 126 (2002).
- [18] J. Nakamura, N. Yamada, K. Kuroki, T. A. Callcott, D. L. Ederer, J. D. Denlinger, and R. C. C. Perera, *Phys. Rev. B* **64**, 174504 (2001).
- [19] T. A. Callcott, L. Lin, G. T. Woods, G. P. Zhang, J. R. Thompson, M. Paranthaman, and D. L. Ederer, *Phys. Rev. B* **64**, 132504 (2001).
- [20] S. Schuppler, E. Pellegrin, N. Nüker, T. Mizokawa, M. Merz, D. A. Arena, J. Dvorak, Y. U. Idzerda, D.-J. Huang, C.-F. Cheng, K.-P. Bohnen, R. Heid, P. Schweiss, and Th. Wolf, *cond-mat/0205230*.
- [21] K.-D. Tsuei, H.-J. Lin, L.-C. Lin, T.-Y. Hou, H.-H. Hsieh, C. T. Chen, N. L. Saini, A. Bianconi, and A. Saccone, *Inter. J. Mod. Phys. B* **16**, 1619 (2002).
- [22] D. B. Tanner, H. L. Liu, M. A. Quijada, A. M. Zibold, H. Berger, R. J. Kelley, M. Onellion, F. C. Chou, D. C. Johnston, J. P. Rice, D. M. Ginsberg, and J. T. Markert, *Physica B* **244**, 1 (1998).
- [23] F. Wooten, in *Optical Properties of Solids* (Academic, New York, 1972).
- [24] For example, B. Gorshunov, C. A. Kuntscher, P. Haas, M. Dressel, F. P. Mena, A. B. Kuz'menko, D. van der Marel, T. Muranaka, and J. Akimitsu, *Eur. Phys. J. B* **21**, 159

(2001).

[25] D. B. Tanner and T. Timusk, in *Physical Properties of High Temperature Superconductors III*, edited by D. M. Ginsberg (World Scientific, Singapore, 1992), p. 363.

[26] S. V. Barabash and D. Stroud, Phys. Rev. B **66**,012509 (2002).

[27] O. de la Peña, A. Aguayo and R. de Coss, Phys. Rev. B **66**,012511 (2002).

FIGURES

FIG. 1. Resistivity $\rho(T)$ of $(\text{Mg}_{1-x}\text{Al}_x)\text{B}_2$. Inset: lattice parameters of $(\text{Mg}_{1-x}\text{Al}_x)\text{B}_2$.

FIG. 2. B K -edge XANES of $(\text{Mg}_{1-x}\text{Al}_x)\text{B}_2$ for $x=0$ to 0.4. The pre-edge peak is associated with the B $2p$ σ hole states.

FIG. 3. Room-temperature optical conductivity spectra of $(\text{Mg}_{1-x}\text{Al}_x)\text{B}_2$.

FIG. 4. The effective number of carriers N_{eff} integrated up to 8000 cm^{-1} vs T_c

FIG. 5. N_{eff} vs x . The experimental results are shown as the solid circles. The theoretical prediction is taken from Ref. 4 and denoted as the solid line. No fitting parameter is adjusted.

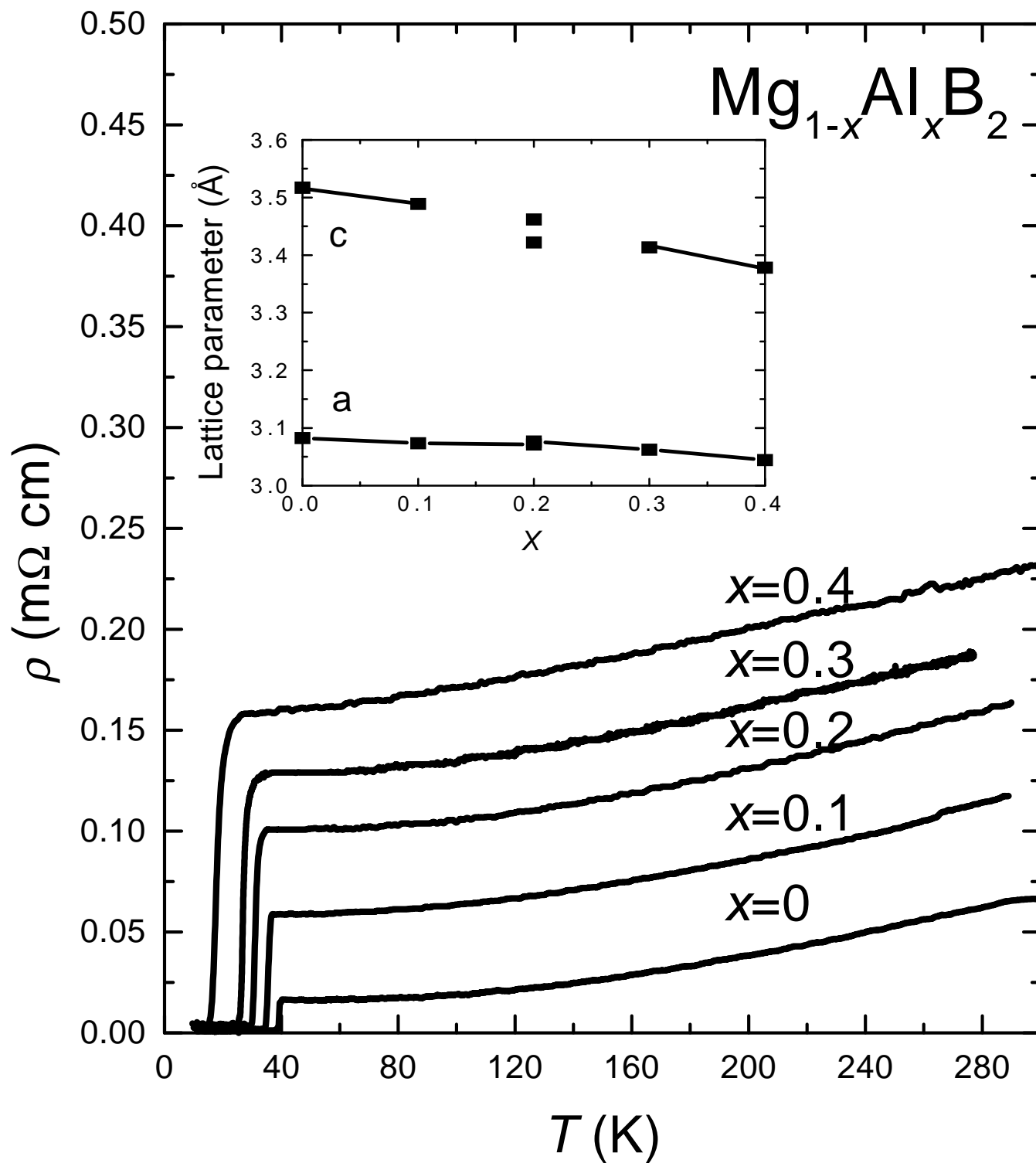


Fig. 1

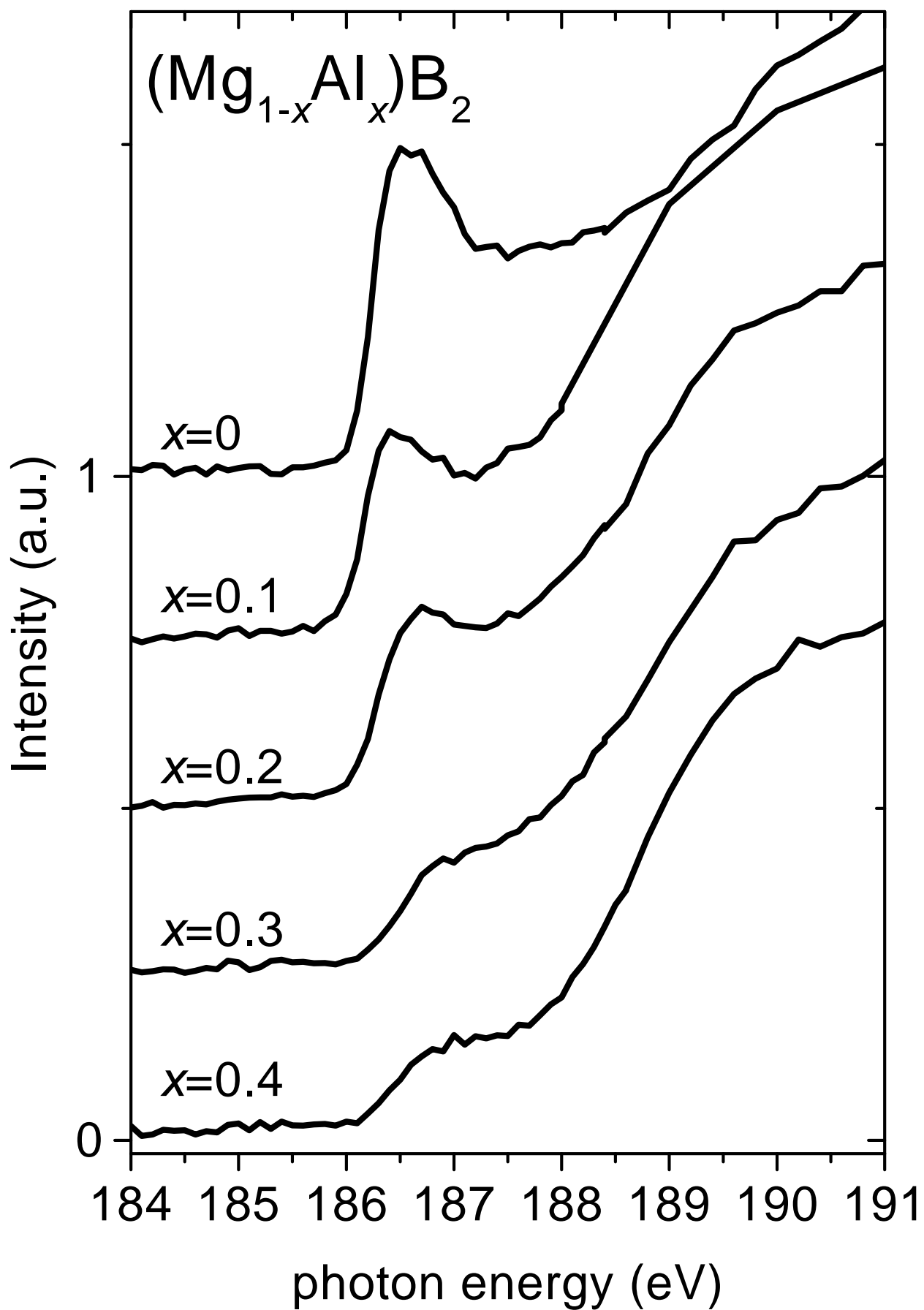


Fig. 2

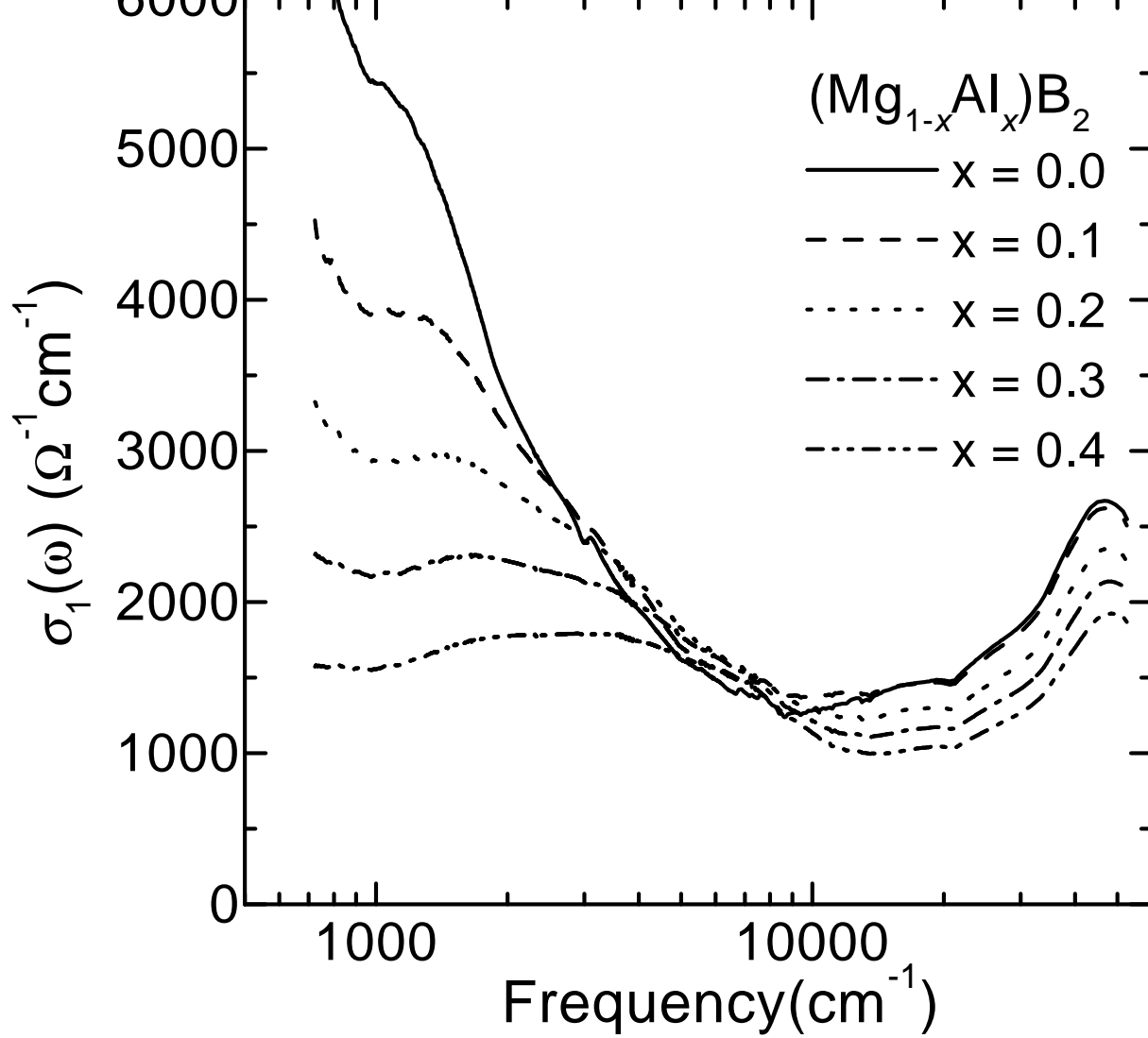


Fig. 3

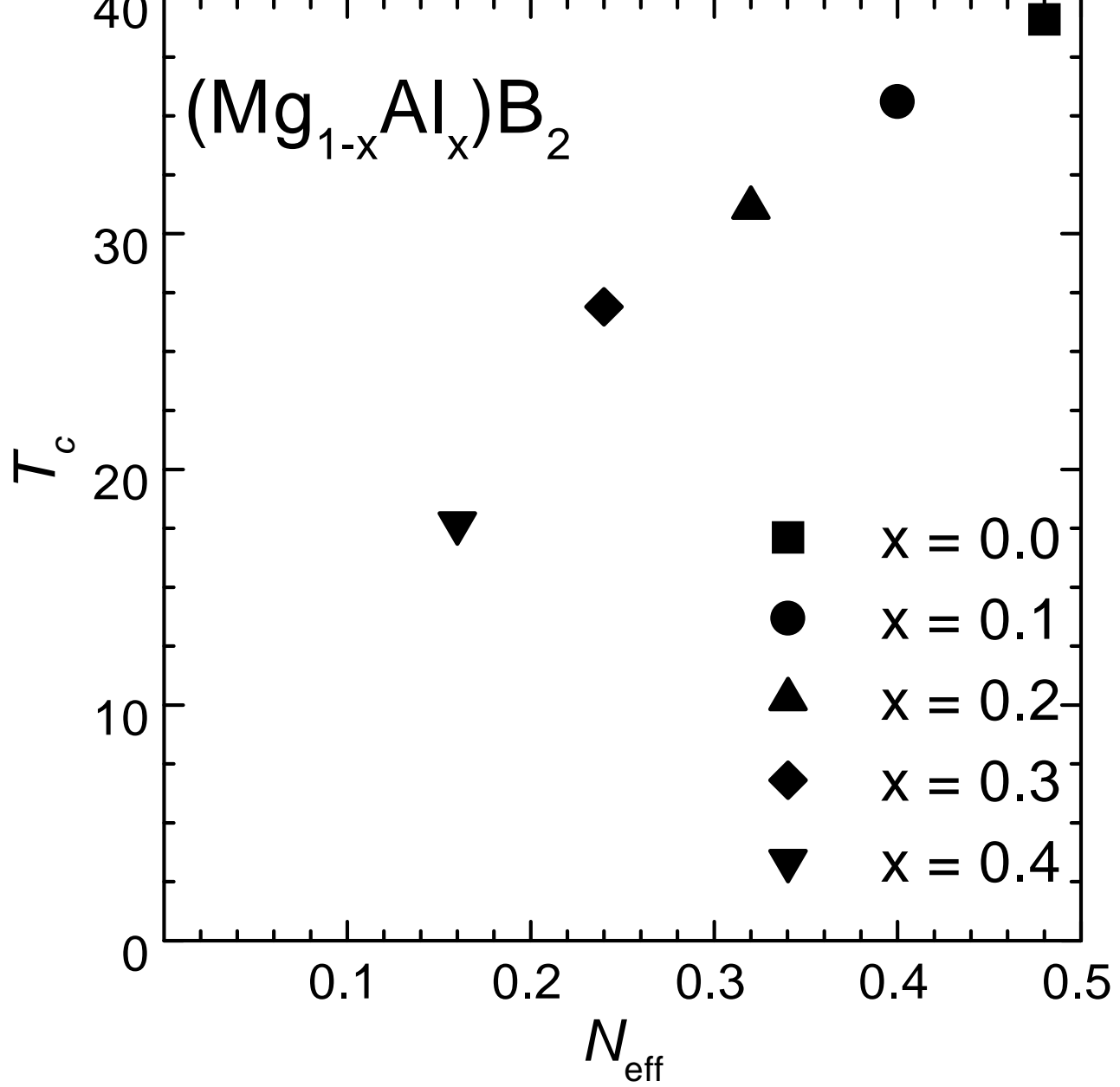


Fig. 4

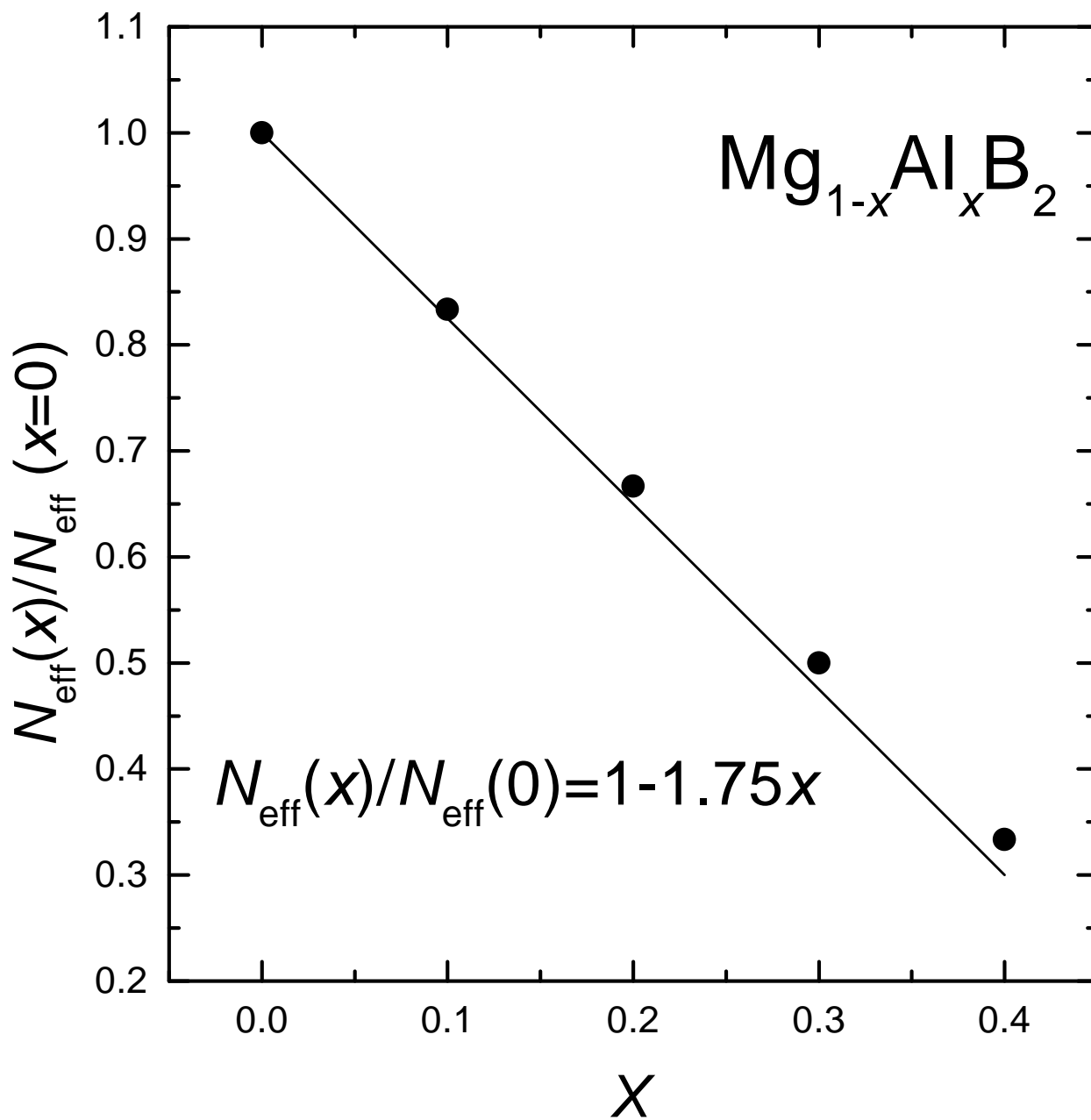


Fig. 5

Yang et al.